Supplementary Fig. S3. Concentration-dependent confirmation of actives that inhibit the DHT-induced formation of AR-TIF2 PPIs identified in the LOPAC screens. **(A)** Concentration-dependent inhibition of DHT-induced AR-TIF2 PPI formation by NR ligands—compounds with incomplete curves. U-2 OS cells were coinfected with the AR-red fluorescent protein (RFP) and TIF2-GFP recombinant adenovirus (rAV) biosensors, 2,500 cells were seeded into the wells of 384-well assay plates, cultured overnight at 37°C, 5% CO_2 and 95% humidity, and then exposed to compounds at the indicated concentrations for 3 h. Cells were then treated with 20 nM DHT for 30 min, fixed and stained with Hoechst, 20× images in three fluorescent channels were acquired on the ImageXpress Ultra (IXU) automated imaging platform, and the AR-TIF2 PPIs were quantified using the translocation enhanced (TE) image analysis module as described previously. The mean ± standard deviation (SD) ($n=3$) percent inhibition of DHT-induced AR-TIF2 PPIs in cells exposed to the indicated concentrations of spironlactone (●), budesonide (○), cortexelone (■), cyproterone (□), mipepristone (▼), or guggulsterone (◇) are presented. Representative experimental data from one of the three independent experiments are shown. **(B)** Images of AR-RFP distribution phenotypes in cells pretreated with non-NR ligands that inhibit DHT-induced AR-TIF2 PPI formation. U-2 OS cells were coinfected with the AR-RFP and TIF2-GFP rAV biosensors, 2,500 cells were seeded into the wells of 384-well assay plates, cultured overnight at 37°C, 5% CO_2, and 95% humidity, and then exposed to compounds at a variety of concentrations for 3 h. Cells were then treated with 20 nM DHT for 30 min, fixed and stained with Hoechst, and 20× images in three fluorescent channels were acquired on the IXU automated imaging platform. Grayscale images of the AR-RFP distribution phenotype of cells preexposed to 50 μM 4-phenyl-3-furoxancarbonitrile (4-P-3-FOCN), 2.5 μM Bay 11-7085, 10 μM parthenolide, 2.5 μM 1-chloro-3-tosylamido-4-phenyl-2-butanone (TPCK) or 2.5 μM N-Carbobenzyloxy-L-phenylalanyl chloromethyl ketone (ZPCK). Grayscale images of the AR-RFP distribution phenotype of the 0.5% dimethyl sulfoxide (DMSO) and 20 nM DHT controls are also presented. Representative images from one of the three independent experiments are shown. **(C)** Images of AR-RFP phenotypes in cells pretreated with NR ligands that inhibit DHT-induced AR-TIF2 PPI formation. U-2 OS cells were coinfected with the AR-RFP and TIF2-GFP rAV biosensors, 2,500 cells were seeded into the wells of 384-well assay plates, cultured overnight at 37°C, 5% CO_2, and 95% humidity, and then exposed to compounds at a variety of concentrations for 3 h. Cells were then treated with 20 nM DHT for 30 min, fixed and stained with Hoechst, and 20× images in three fluorescent channels were acquired on the IXU automated imaging platform. Grayscale images of the AR-RFP distribution phenotype of cells preexposed to 10 μM mifepristone, 10 μM 17-alpha-hydroxyprogesterone (17-α-H-PG), 10 μM nilutamide, 10 μM spironlactone, 50 μM gugglesterone, 10 μM cyproterone, 50 μM 2-methoxyestradiol (2-MOED), 50 μM budesonide, 50 μM cotexelone, or 50 μM estrone are presented. Grayscale images of the AR-RFP distribution phenotype of the 0.5% DMSO and 20 nM DHT controls are also presented. Representative images from one of the three independent experiments are shown.

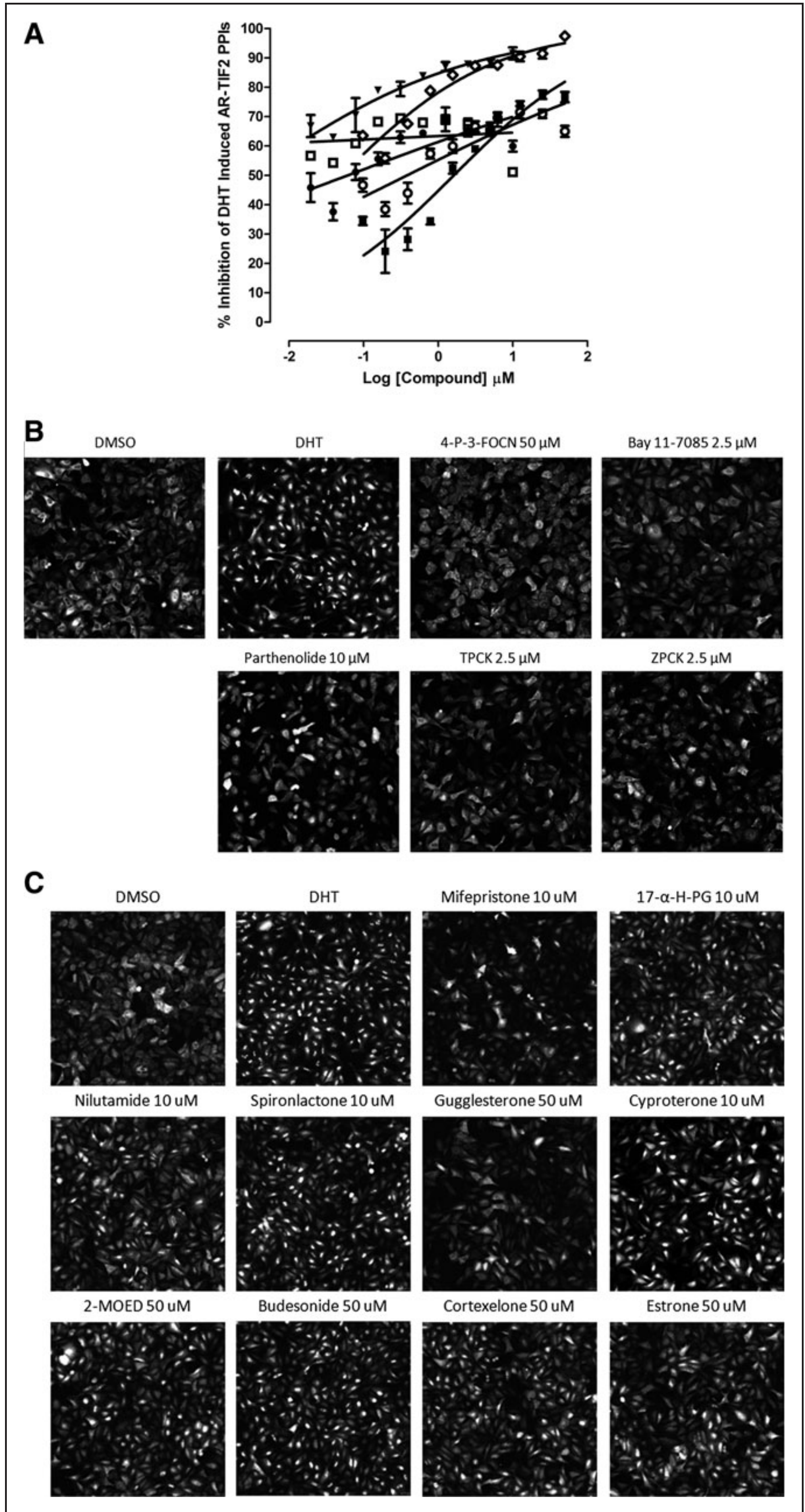
A
% Inhibition of DHT Induced AR-TIF2 PPIs
Log [Compound] μM
B
DMSO
DHT
4-P-3-FOCN 50 μM
Bay 11-7085 2.5 μM
Parthenolide 10 μM
TPCK 2.5 μM
ZPCK 2.5 μM
C
DMSO
DHT
Mifepristone 10 uM
17-α-H-PG 10 uM
Nilutamide 10 uM
Spironlactone 10 uM
Gugglesterone 50 uM
Cyproterone 10 uM
2-MOED 50 uM
Budesonide 50 uM
Cortexelone 50 uM
Estrone 50 uM